

Weakly- and Semi-Supervised Learning of a Deep Convolutional Network for Semantic Image Segmentation

George Papandreou

Google, Inc.

GPAPAN@GOOGLE.COM

Liang-Chieh Chen

Univ. of California, Los Angeles

LCCHEN@CS.UCLA.EDU

Kevin Murphy

Google, Inc.

KPMURPHY@GOOGLE.COM

Alan L. Yuille

Univ. of California, Los Angeles

YUILLE@STAT.UCLA.EDU

Abstract

Deep convolutional neural networks (DCNNs) trained on a large number of images with strong pixel-level annotations have recently significantly pushed the state-of-art in semantic image segmentation. We study the more challenging problem of learning DCNNs for semantic image segmentation from either (1) weakly annotated training data such as bounding boxes or image-level labels or (2) a combination of few strongly labeled and many weakly labeled images, sourced from one or multiple datasets. We develop methods for semantic image segmentation model training under these weakly supervised and semi-supervised settings. Extensive experimental evaluation shows that the proposed techniques can learn models delivering state-of-art results on the challenging PASCAL VOC 2012 image segmentation benchmark, while requiring significantly less annotation effort.

demonstrating state-of-the-art performance on the challenging Pascal VOC 2012 segmentation benchmark (Chen et al., 2014b; Mostajabi et al., 2014; Long et al., 2014). The network parameters are tuned to optimize the pixel-wise segmentation accuracy and typically strong, pixel-wise annotations are employed to learn the models. However, it is very labor-intensive to collect the full annotations for thousands or millions of images. We study the problem of harnessing weaker annotations in learning DCNN segmentation models, focusing on the state-of-art DeepLab-CRF model of Chen et al. (2014b). Weak annotations, such as image-level labels (*i.e.*, information about which object classes are present) or bounding boxes (*i.e.*, coarse object locations) are far easier to collect than detailed pixel-level annotations.

1. Introduction

Semantic image segmentation refers to the problem of assigning a semantic label to every pixel in the image and is a significant component of scene understanding systems. Deep Convolutional Neural Networks (DCNNs) have been successfully applied to this task (Farabet et al., 2013; Pinheiro & Collobert, 2014a; Eigen & Fergus, 2014), recently

Related Work Training semantic image segmentation models using solely image-level labels for is a challenging problem that has attracted much interest in the literature (Duygulu et al., 2002; Verbeek & Triggs, 2007; Vezhnevets & Buhmann, 2010; Vezhnevets et al., 2011; 2012; Xu et al., 2014). These earlier works have shown encouraging results on some datasets but have not been demonstrated on the challenging PASCAL VOC 2012 benchmark. Some recent works use modern DCNN architectures and develop Multiple Instance Learning (MIL) based methods appropriate for the image-level weakly-supervised setting, but report results far lagging the strongly-supervised state-of-art (Pathak et al., 2014; Pinheiro & Collobert, 2014b). Similar MIL-based approaches have also been employed in training image classification models but their localization performance has not been directly evaluated (Oquab et al., 2014; Papandreou et al., 2014).

The first two authors contributed equally to this work.

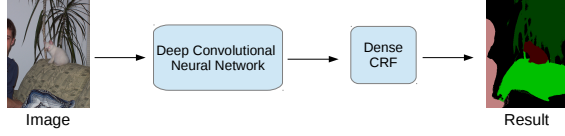


Figure 1. Overview of the DeepLab-CRF model.

Several previous works have harnessed bounding box annotations as another source of weak supervision in training image segmentation models [Xia et al. \(2013\)](#); [Guillumin et al. \(2014\)](#); [Chen et al. \(2014a\)](#); [Zhu et al. \(2014\)](#). Bounding box annotations are also commonly used in foreground/background image segmentation ([Lempitsky et al., 2009](#); [Rother et al., 2004](#)). Combining few strong annotations and a large number of weak annotations in a semi-supervised setting is another emerging research direction ([Hoffman et al., 2014](#)).

Contributions Our paper develops new methods and presents systematic experimental evaluations in harnessing weak annotations for training a DCNN semantic image segmentation model. In particular:

1. We present an EM algorithm for training with image-level labels, applicable to both pure weakly-supervised and semi-supervised settings. This EM algorithm performs better than the MIL methods.
2. We develop a method to estimate foreground object segments from bounding boxes. Models trained with this inferred segmentations yield significantly better results than models trained with the whole bounding box area as object annotation.
3. We develop a semi-supervised training method integrating our EM algorithm and demonstrate excellent performance when combining a small number of pixel-level annotated images with a large number of image-level annotated images, nearly matching the results achieved when all training images have pixel-level annotations.
4. We show that combining weak or strong annotations across datasets yields significantly better results. In particular, we set the new state-of-art in the PASCAL VOC 2012 segmentation benchmark with 70.4% IOU performance by combining annotations from the PASCAL and MS-COCO datasets.

2. Proposed Methods

2.1. The DeepLab-CRF Model for Semantic Image Segmentation

Our starting point is the recently proposed DeepLab model for semantic image segmentation of [Chen et al. \(2014b\)](#), illustrated in Figure 1. This model applies a deep CNN to an image in a sliding window fashion to generate score maps for each pixel location $i = 1, \dots, N$

$$f_i(x_i; \theta), \quad \text{with} \quad P_i(x_i; \theta) \propto \exp(f_i(x_i; \theta)) \quad (1)$$

where $x_i \in \mathcal{L}$ is the i -th pixel’s assignment to the discrete candidate semantic label set \mathcal{L} , θ is the vector of CNN model parameters, and normalization ensures that $\sum_{x_i \in \mathcal{L}} P_i(x_i; \theta) = 1$ for every pixel i . Computation sharing in the convolutional layers by means of the hole algorithm and careful network crafting as detailed in [Chen et al. \(2014b\)](#) make the method computationally efficient.

Score map post-processing by means of a fully-connected CRF (Dense CRF) ([Krähenbühl & Koltun, 2011](#)) significantly improves segmentation performance near object boundaries. Specifically, [Chen et al. \(2014b\)](#) integrate into their system the fully connected CRF model of [Krähenbühl & Koltun \(2011\)](#). The model employs the energy function

$$E(x) = \sum_i f_i(x_i) + \sum_{ij} g_{ij}(x_i, x_j) \quad (2)$$

where x_i is the i -th pixel’s label assignment. The additional pairwise potential $g_{ij}(x_i, x_j) = \mu(x_i, x_j) \sum_{m=1}^K w_m \cdot k_m(\mathbf{y}_i, \mathbf{y}_j)$, where $\mu(x_i, x_j) = 1$ if $x_i \neq x_j$, and zero otherwise (*i.e.*, Potts Model). There is one such term for each pair of pixels i and j in the image no matter how far from each other they lie. Each k_m is the Gaussian kernel depends on features (denoted as \mathbf{y}) extracted for pixel i and j and is weighted by parameter w_m . [Chen et al. \(2014b\)](#) employ bilateral position and color terms, specifically:

$$w_1 \exp \left(-\frac{\|p_i - p_j\|^2}{2\sigma_\alpha^2} - \frac{\|I_i - I_j\|^2}{2\sigma_\beta^2} \right) + w_2 \exp \left(-\frac{\|p_i - p_j\|^2}{2\sigma_\gamma^2} \right) \quad (3)$$

where the first kernel depends on both pixel positions (denoted as p) and pixel color intensities (denoted as I), and the second kernel only depends on pixel positions. The Gaussian form of potentials allows for rapid mean-field inference ([Krähenbühl & Koltun, 2011](#)), despite the full connectivity of the model’s factor graph. The parameters σ_α , σ_β and σ_γ control the “scale” of the Gaussian kernels.

2.2. Model Training Using Fully Annotated Images

The network parameters θ are trained by stochastic gradient descent (SGD) so as to minimize the average log-loss

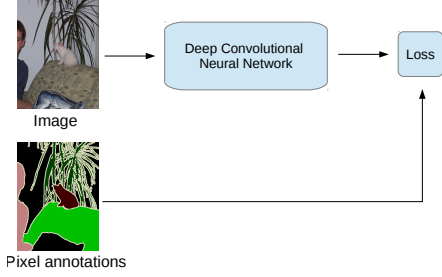


Figure 2. DeepLab model training from fully annotated images.

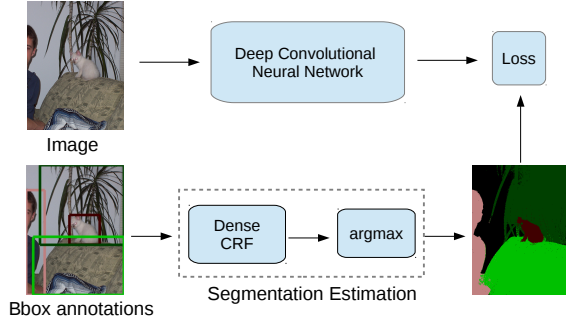


Figure 3. DeepLab model training using bounding box data and automated foreground/ background segmentation.

$$L(\theta) = \frac{1}{N} \sum_{i=1}^N \log P_i(l_i; \theta) \quad (4)$$

between the model predictions and the pixel-wise ground truth labels $\{l_i\}_{i=1}^N$, as illustrated in Figure 2. Similarly to Chen et al. (2014b), we do not include the Dense CRF module into the training pipeline for simplicity and speed during training.

Learning the DeepLab-CRF model on fully annotated images works very well in practice, yielding state-of-art performance (66.4% IOU) in the challenging PASCAL VOC 2012 image segmentation benchmark. However, the need for detailed annotations makes it harder to gather very large training datasets and makes it difficult to train the model for new domains, especially when the number of candidate labels (*i.e.*, the cardinality of the label set \mathcal{L}) is large.

2.3. Model Training Using Bounding Box Weak Annotations

Collecting bounding box annotations is significantly easier compared to pixel-level ground truth segmentations. We have explored two alternative methods for training the DeepLab segmentation model from bounding boxes with object-level labels. In both methods we estimate dense segmentation maps from the bounding box annotation as a pre-processing step, then employ the training procedure

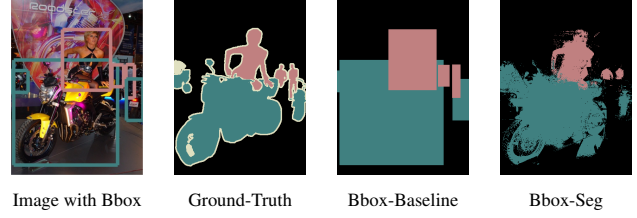


Figure 4. Estimated segmentation from bounding box annotation.

of Sec. 2.2 treating these estimated labels as ground-truth, as illustrated in Fig. 3.

The first *Bbox-Baseline* method amounts to simply considering each pixel within the bounding box as positive example for the respective object class. Ambiguities are resolved by assigning pixels that belong to multiple bounding boxes to the one that has the smallest area.

The bounding boxes fully surround objects but also contain background pixels that contaminate the training set with false positive examples for the respective object classes. To filter out these background pixels, we have also explored a second *Bbox-Seg* method in which we perform automatic foreground/background segmentation in the spirit of Rother et al. (2004). We assign to pixels in the foreground segment the label of the bounding box and to pixels in the background segment the background label. For the foreground/background segmentation we employ once more the Dense CRF model. More specifically, we constrain the center area of the bounding box ($\alpha\%$ of pixels within the box) to be foreground, while we constrain pixels outside the bounding box to be background. We implement this by appropriately setting the unary terms of Eq. (1). The Dense CRF is then applied to infer the label for pixels in between. We cross-validate the Dense CRF parameters so as to maximize segmentation accuracy in a small held-out set of fully-annotated images.

Examples of estimated segmentations with the two methods are shown in Fig. 4.

2.4. Model Training Using Weak Image-Level Labels

Training the DeepLab segmentation model using only image-level labels is significantly more challenging.

Previous MIL Approaches and their Limitations Previous related CNN literature employs multiple instance learning variants to address the weak supervision problem, but has demonstrated limited success in learning accurate segmentation models.

In particular, recent work by Pathak et al. (2014) attempts to learn the CNN parameters for the segmentation model by adapting an MIL formulation previously employed for

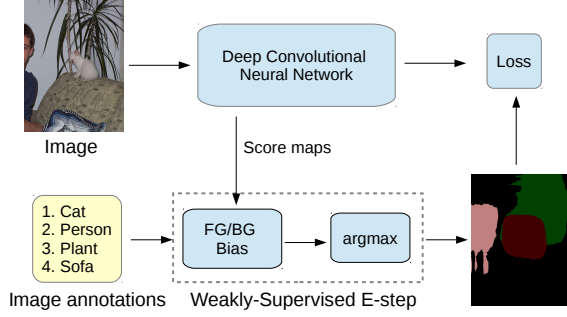


Figure 5. DeepLab model training using image-level labels by weakly-supervised Expectation-Maximization.

image classification tasks (Oquab et al., 2014; Papandreou et al., 2014). More specifically, during training they compute an aggregate image-level response for each class x as the maximum class score across all pixel positions i

$$\bar{f}(x; \theta) = \max_i f_i(x; \theta) \quad \text{and} \quad \bar{P}(x; \theta) \propto \exp(\bar{f}(x; \theta)) \quad (5)$$

which is then combined with the image-level ground-truth label l to compute the whole-image loss $\bar{L}(\theta) = \log \bar{P}(l; \theta)$. A similar formulation with softmax instead of max aggregation has been pursued before by Pinheiro & Collobert (2014b).

There are several limitations to this MIL-based approach to the image segmentation problem. *First*, the model does not explicitly encourage good localization during training, since it suffices to give strong response for the correct class anywhere within the image. *Second*, MIL does not promote good object coverage. For example, it is often sufficient to learn a good face detector to reliably determine whether an image contains a person. However, this face detector will give false-negative responses on the rest of the human body and is thus not appropriate for segmenting whole persons. *Third*, this MIL formulation does not incorporate competition across channels, with maximum responses of multiple classes potentially coming from the same image position. The model is thus allowed to ignore a large portion of the image content during training. These issues have undermined the success of previous CNN/MIL approaches to image segmentation and the performance of such models trained on weak labels significantly lags their counterparts trained on pixel-level annotations, as explained in Sec. 3.

Weakly Supervised Expectation-Maximization We propose an alternative training procedure based on the Expectation-Maximization (EM) algorithm adapted to our weakly-labeled image segmentation setting.

In this setting, we consider the pixel-level semantic labels $\{l_i\}_{i=1}^N$ as latent variables. We incorporate the image-level semantic labels as side-information that biases the E-step of

Algorithm 1 Weakly-Supervised EM (fixed bias version)

Input: CNN parameters θ and biases $c_f, c_b > 0$.

E-Step: For each image position i

- 1: $\hat{f}_i(x_i; \theta) = f_i(x_i; \theta) + c_f$, if x_i is FG label \triangleright FG bias
- 2: $\hat{f}_i(x_i; \theta) = f_i(x_i; \theta) + c_b$, if x_i is BG label \triangleright BG bias
- 3: $\hat{f}_i(x_i; \theta) = f_i(x_i; \theta)$, if label x_i not present
- 4: $\hat{l}_i = \operatorname{argmax}_{x_i \in \mathcal{L}} \hat{f}_i(x_i; \theta)$ \triangleright Hard assignments

M-Step:

- 5: $\hat{L}(\theta) = \frac{1}{N} \sum_{i=1}^N \log P_i(\hat{l}_i; \theta)$ \triangleright Expected loss
 - 6: Update θ by SGD with momentum on $\hat{L}(\theta)$
-

the EM algorithm, as detailed in Algorithm 1 and illustrated in Fig. 5. The fixed positive foreground and background biases c_f and c_b in this *EM-Fixed* algorithm favor the score maps corresponding to labels present in the image, incorporating the prior information carried by the image-level weak annotation. A similar method has been employed before (Lu et al., 2013). Also see Cour et al. (2011) for an alternative approach. We have obtained better results by choosing $c_f > c_b$, slightly favoring foreground objects over the background to encourage higher foreground object coverage. Notably, the E-step assigns a label to every image pixel and thus the model parameters are updated during the M-step to better explain the whole image content.

We have also experimented with an adaptive *EM-Adapt* variant of Algorithm 1 in which the biases are chosen adaptively per image so as a pre-defined proportion of the image area is assigned to the foreground object class, similarly to Kuck & de Freitas (2005). This acts as a hard constraint that explicitly prevents the background score from prevailing in the whole image, also promoting higher foreground object coverage. We have found this adaptive variant to perform better in the purely weakly supervised scenario, whereas the fixed bias variant works best in the semi-supervised training scenario discussed next.

2.5. Semi-Supervised Model Training Using Both Fully and Weakly Annotated Images

In practice, we often have access to a large number of weakly image-level annotated images and can only afford to procure detailed pixel-level annotations for a small fraction of these images. We propose to handle this hybrid semi-supervised training scenario by combining the methods presented in the previous sections, as illustrated in Figure 6. In SGD training of our deep CNN models, we bundle to each mini-batch a fixed proportion of strongly/weakly annotated images, and employ the fixed-bias version of our weakly-supervised EM algorithm in estimating at each iteration the latent semantic segmentations for the weakly annotated images. We demonstrate in Sec. 3 that one needs to annotate in detail at the pixel-level only a small part of the

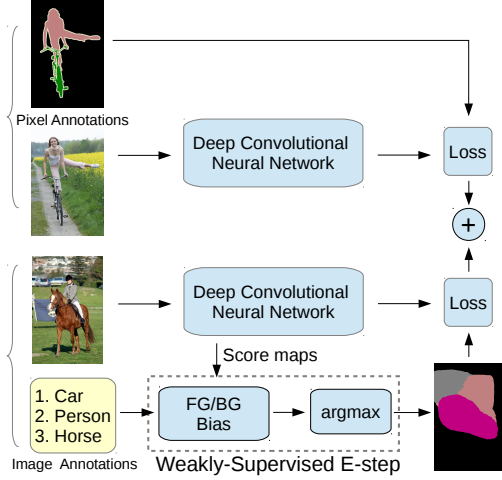


Figure 6. DeepLab model training on a union of full (strong labels) and image-level (weak labels) annotations.

dataset and use image-level labels for the remaining part to achieve the same level of performance with a DeepLab model trained with the whole dataset fully annotated.

3. Experimental Evaluation

3.1. Experimental Protocol

Dataset The proposed training methods are evaluated on the PASCAL VOC 2012 segmentation benchmark (Everingham et al., 2014), consisting of 20 foreground object classes and one background class. The performance is measured in terms of pixel intersection-over-union (IOU) averaged across the 21 classes. The segmentation part of the original PASCAL VOC 2012 dataset contains 1464 (*train*), 1449 (*val*), and 1456 (*test*) images for training, validation, and test, respectively. In some experiments we also use the extra annotations provided by Hariharan et al. (2011), resulting in augmented sets of 10,582 (*train.aug*) and 12,031 (*trainval.aug*) images. We have also experimented with the large MS-COCO 2014 dataset (Lin et al., 2014), which contains 123,287 images in its *trainval* set. The MS-COCO 2014 dataset has 80 foreground object classes and one background class and is also annotated at the pixel level. Evaluation of our proposed methods is primarily conducted on the PASCAL VOC 2012 *val* set but we also report results of selected method variants submitted to the official PASCAL VOC 2012 server, which evaluates results on the *test* set (whose annotations are not released).

Training We employ our proposed training methods to learn the DCNN component of the DeepLab-CRF model of Chen et al. (2014b). We start with the Imagenet (Deng et al., 2009) pretrained VGG-16 network of Simonyan & Zisserman (2014), modified as described in Chen et al. (2014b). In SGD training, we use a mini-batch of 20 im-

Table 1. DeepLab-CRF VOC 2012 *val* IOU (%) results using bounding box weak annotations vs. strong annotation (Sec. 3.3).

Bbox-Baseline	Bbox-Seg	Strong
52.5	58.5	63.9

Table 2. DeepLab-CRF VOC *val* IOU (%) results with image-level weak annotations in training vs. previous methods (Sec. 3.4).

MIL1	MIL2	MIL2-ILP	EM-Fixed	EM-Adapt
20.5	17.8	32.6	20.8	38.2

ages and initial learning rate of 0.001 (0.01 for the final classifier layer), multiplying the learning rate by 0.1 after a fixed number of iterations. We use momentum of 0.9 and a weight decay of 0.0005. Fine-tuning our network on PASCAL VOC 2012 takes about 12 hours on a NVIDIA Tesla K40 GPU. Our implementation is based on the publicly available Caffe software (Jia et al., 2014).

Similarly to Chen et al. (2014b), we decouple the DCNN and Dense CRF training stages and learn the CRF parameters by cross validation so as to maximize IOU segmentation accuracy in a held-out set of 100 Pascal *val* fully-annotated images. We use 10 mean-field iterations for Dense CRF inference (Krähenbühl & Koltun, 2011).

Weak annotations In order to simulate the situations where only weak annotations are available and to have fair comparisons (e.g., use the same images for all settings), we generate the weak annotations from the pixel-level annotations. The image-level labels are easily generated by summarizing the pixel-level annotations, while the bounding box annotations are produced by drawing rectangles tightly containing each object instance (PASCAL VOC 2012 also provides instance-level annotations) in the dataset.

3.2. Model Training Using Fully Annotated Images

The performance of the DeepLab-CRF model trained with strong pixel-level annotations sets a target upper bound which we try to reach with the proposed algorithms for weakly- or semi-supervised training. In reproducing the results of (Chen et al., 2014b) on PASCAL VOC 2012 *val*, we have achieved a *DeepLab-CRF(Strong)* IOU score of **63.9%** (they report a score of 63.7 in their Table 1a).

3.3. Model Training Using Bounding Box Weak Annotations

In this experiment we train the DeepLab-CRF model using the 10,582 PASCAL VOC 2012 *train.aug* bounding box annotations, generated as described in Sec. 3.1 above. We estimate the training set segmentations in a pre-processing step using the *Bbox-Baseline* and *Bbox-Seg* methods described in Sec. 2.3.

We assume that we also have access to 100 fully-annotated PASCAL VOC 2012 *val* images which we have used to

Table 3. DeepLab-CRF VOC 2012 *val* IOU (%) results using both strong pixel-level and weak image-level annotations (Sec. 3.5).

#Strong	#Weak	DeepLab-CRF	Scenario
0	10,582	20.8	Weak-EM-Fixed
0	10,582	38.2	Weak-EM-Adapt
200	10,382	47.6	Semi
500	10,082	56.9	
750	9,832	58.8	
1,000	9,582	60.5	
1,464	5,000	60.5	Semi
1,464	9,118	61.9	
1,464	0	57.6	Strong
10,582	0	63.9	

cross-validate the value of the single *Bbox-Seg* parameter α (percentage of the center bounding box area constrained to be foreground). We varied α from 20% to 80%, finding that using $\alpha = 20\%$ maximizes the accuracy in terms of IOU in recovering the ground truth foreground from the bounding box.

The PASCAL VOC 2012 *val* performance achieved after training the DeepLab-CRF model on the segmentations obtained by the *Bbox-Baseline* and *Bbox-Seg* is reported in Tab. 1. We see that *Bbox-Seg* improves over *Bbox-Baseline* by nearly 6% but still lags by 5.5% compared to training with the strong pixel-level annotation.

3.4. Model Training Using Weak Image-Level Labels

We proceed with evaluating our proposed methods in training the DeepLab-CRF model using just image-level weak annotations from the 10,582 PASCAL VOC 2012 *train_aug* set, generated as described in Sec. 3.1 above. We report the *val* performance of our two weakly-supervised EM variants described in Sec. 2.4. In the *EM-Fixed* variant we use $c_f = 6$ and $c_b = 5$ as fixed foreground and background biases. We found the results to be quite sensitive to the difference $c_f - c_b$ but not very sensitive to their absolute values. In the adaptive *EM-Adapt* variant we constrain at least 40% of the image area to be assigned to background and at least 20% of the image area to be assigned to foreground (as specified by the weak label set).

The PASCAL VOC 2012 *val* performance achieved after training the DeepLab-CRF model with this weakly-supervised EM algorithm are reported in Tab. 2. This table also contains results obtained by the previous MIL-based methods *MIL1* (Pathak et al., 2014) and *MIL2*, *MIL2-ILP* (Pinheiro & Collobert, 2014b). Note that the numbers are not directly comparable because Pathak et al. (2014) evaluates on the VOC 2011 *val* and Pinheiro & Collobert (2014b) train the parameters of their CNN models on the Imagenet dataset.

We observe that *EM-Fixed* performs poorly on this challenging task, at the same level as the previous *MIL1* and

Table 4. DeepLab-CRF VOC 2012 *val* IOU (%) using strong annotations for all 10,582 *train_aug* PASCAL images and a varying number of strong and weak MS-COCO annotations (Sec. 3.6).

#Strong	#Weak	DeepLab-CRF	Scenario
0	0	63.9	PASCAL-only
0	123,287	64.4	Weak-EM-Fixed
5,000	118,287	66.5	Semi-Cross-Joint
5,000	0	64.9	Strong-Cross-Joint
123,287	0	68.0	Strong-Cross-Pretrain
123,287	0	68.0	Strong-Cross-Joint

MIL2 methods. Similarly to them, we observed that the *EM-Fixed* model had particularly difficulty in balancing the scores of the foreground and background classes, often producing all-background segmentations. The *MIL2-ILP* method partially alleviates this problem by departing from the pure MIL formulation, also incorporating image-level classification scores during training. Our *EM-Adapt* method performed the best by explicitly enforcing both background and foreground labels to emerge in the estimation process. However, its performance at 38.2% significantly lags the target 63.9% goal of the strongly-supervised model trained on pixel-level annotations.

3.5. Semi-Supervised Model Training Using Both Fully and Weakly Annotated Images

We next examine to what extent weak image-level annotations can complement strong pixel-level annotations in training the DeepLab-CRF model, using the semi-supervised learning methods of Sec. 2.5. In this *Semi* setting we employ the strong annotations of a subset of PASCAL VOC 2012 *train* set and use just the weak image-level labels from another non-overlapping subset of the *train_aug* set. We perform segmentation inference for the images that only have image-level labels by means of *EM-Fixed*. In Tab. 3 we report the results obtained by varying the sizes of the strong and weak annotation sets, also including for comparison the results of pure weakly-supervised and strongly-supervised learning.

We observe that including even a few hundreds of strongly annotated images in the semi-supervised setting significantly improves the performance compared to the pure weakly-supervised baseline. We also observe that using just 1,464 strongly annotated images (13.8% of the *train_aug* set) along with the remaining weakly annotated images suffices to reach performance 61.9%, only 2% lower than the result obtained by pure strongly-supervised training on all 10,582 *train_aug* images. Note that only using the 1,464 strongly annotated images in the *train* set and no weakly annotated images performs significantly worse at 57.6%, demonstrating the significant benefits of the semi-supervised setting.

Table 5. Benchmark IOU (%) results on PASCAL VOC 2012 test. Links to the PASCAL evaluation server are included in the PDF.

Method	bkg	aero	bike	bird	boat	bottle	bus	car	cat	chair	cow	table	dog	horse	mbike	person	plant	sheep	sofa	train	tv	mean
Hypercolumn-SDS	88.9	68.4	27.2	68.2	47.6	61.7	76.9	72.1	71.1	24.3	59.3	44.8	62.7	59.4	73.5	70.6	52.1	63.0	38.1	60.0	54.1	59.2
MSRA-CFM	-	75.7	26.7	69.5	48.8	65.6	81.0	69.2	73.3	30.0	68.7	51.5	69.1	68.1	71.7	67.5	50.4	66.5	44.4	58.9	53.5	61.8
FCN-8s	-	76.8	34.2	68.9	49.4	60.3	75.3	74.7	77.6	21.4	62.5	46.8	71.8	63.9	76.5	73.9	45.2	72.4	37.4	70.9	55.1	62.2
TTI-Zoomout-16	89.8	81.9	35.1	78.2	57.4	56.5	80.5	74.0	79.8	22.4	69.6	53.7	74.0	76.0	76.6	68.8	44.3	70.2	40.2	68.9	55.3	64.4
DeepLab-CRF	92.1	78.4	33.1	78.2	55.6	65.3	81.3	75.5	78.6	25.3	69.2	52.7	75.2	69.0	79.1	77.6	54.7	78.3	45.1	73.3	56.2	66.4
Weak-EM-Adapt	76.4	37.0	17.6	38.2	26.6	37.1	51.9	43.3	48.1	16.8	44.6	27.9	46.5	46.2	46.6	30.3	28.9	42.0	30.0	43.8	39.3	39.0
Weak-Bbox-Baseline	82.9	43.6	22.5	50.5	45.0	62.5	76.0	66.5	61.2	25.3	55.8	52.1	56.6	48.1	60.1	58.2	49.5	58.3	40.7	62.3	61.1	54.2
Weak-Bbox-Seg	89.9	69.3	28.2	71.9	43.4	59.7	74.3	69.0	76.7	23.5	64.6	47.1	71.0	64.0	72.8	72.4	50.4	72.0	40.2	63.4	44.5	60.4
Semi (1,464 strong)	91.4	77.3	38.2	73.9	47.6	57.9	80.0	76.4	74.7	22.8	70.0	42.0	70.9	71.9	79.1	70.7	47.8	77.1	36.1	68.1	59.8	63.5
Semi (2,913 strong)	92.3	81.3	43.8	78.3	50.2	60.4	81.2	77.5	77.5	26.8	70.8	47.0	74.8	73.0	80.8	76.0	50.8	78.0	39.7	72.9	60.9	66.4
Strong-Cross-Joint	93.2	85.3	36.2	84.8	61.2	67.5	84.7	81.4	81.0	30.8	73.8	53.8	77.5	76.5	82.3	81.6	56.3	78.9	52.3	76.6	63.3	70.4

3.6. Exploiting Annotations Across Datasets

Finally, we present experiments leveraging the 81-label MS-COCO dataset as an additional source of data in learning the DeepLab model for the 21-label PASCAL VOC 2012 segmentation task. We consider three scenarios:

- *Strong-Cross-Pretrain*: Pre-train DeepLab on MS-COCO, then replace the top-level network weights and fine-tune on Pascal VOC 2012, using pixel-level annotation in both datasets.
- *Strong-Cross-Joint*: Jointly train DeepLab on Pascal VOC 2012 and MS-COCO, sharing the top-level network weights for the common classes, using pixel-level annotation in both datasets.
- *Semi-Cross-Joint*: Jointly train DeepLab on Pascal VOC 2012 and MS-COCO, sharing the top-level network weights for the common classes, using the pixel-level labels from PASCAL and varying the number of pixel- and image-level labels from MS-COCO.

In all cases we use strong pixel-level annotations for all 10,582 *train_aug* PASCAL images.

We report our results on the PASCAL VOC 2012 *val* in Tab. 4, also including for comparison our best PASCAL-only 63.9% result exploiting all 10,582 strong annotations as a baseline. When we employ the weak MS-COCO annotations (*Weak-EM-Fixed*) we obtain 64.4% IOU, a marginal 0.5% improvement over the PASCAL-only baseline. Using strong labels from 5,000 MS-COCO images (4.0% of the MS-COCO dataset) and weak labels from the remaining MS-COCO images in the *Semi-Cross-Joint* semi-supervised scenario yields 66.5%, a significant 2.6% boost over the baseline. This *Semi-Cross-Joint* result is also 1.6% better than the 64.9% performance obtained using only the 5,000 strong and no weak annotations from MS-COCO. As expected, our best results are obtained by using all 123,287 strong MS-COCO annotations. Both *Strong-Cross-Pretrain* and *Strong-Cross-Joint* yield 68.0% in this scenario. We observe that cross-dataset augmentation significantly improves over the best PASCAL-only result. Using only a small portion of pixel-level annotations

and a large portion of image-level annotations in the semi-supervised setting suffices to reap most of this benefit.

3.7. Qualitative Segmentation Results

We provide in Fig. 7 visual comparisons of the results obtained by the DeepLab-CRF model learned with the proposed training methods. The segmentation result of the model trained on only weak labels (*Weak-EM-Adapt*) does capture the presence of objects but is rather noisy. In the bounding box training scenario, training with inferred segmentations (*Bbox-Seg*) significantly improves the localization accuracy over *Bbox-Baseline*. Using 1,464 strong and 9,118 weak PASCAL annotations in the *Semi (1,464 strong)* experiment yields significantly better results. We obtain the visually best segmentation results when using all available strong annotations from both the PASCAL and MS-COCO datasets (*Strong-Cross-Joint*).

3.8. Evaluation on PASCAL VOC 2012 Test Set and Comparison with State-of-Art

We report in Tab. 5 our DeepLab-CRF results on the PASCAL VOC 2012 *test* set, evaluating the performance of the proposed training methods on the official segmentation benchmark. We also compare our results with other leading models from the PASCAL leaderboard, namely *Hypercolumn-SDS* (Hariharan et al., 2014), *MSRA-CFM* (Dai et al., 2014), *FCN-8s* (Long et al., 2014), and *TTI-Zoomout-16* (Mostajabi et al., 2014).

The *DeepLab-CRF* model (Chen et al., 2014b) trained with all PASCAL *trainval_aug* strong pixel-level annotations is the current state-of-art with 66.4% IOU performance, which we aim to reach with weaker annotation during training. Using only the weak image-level PASCAL *trainval_aug* labels, the proposed *Weak-EM-Adapt* method yields 39.0%. When we have access to weak bounding box annotation, we can do much better, achieving 54.2% with *Weak-Bbox-Baseline* and 60.4% with *Weak-Bbox-Seg*, only 6% worse than the target performance. We perform even better when we only have access to a small subset of pixel-level annotated images and use just the image-level annotations of the remaining *trainval_aug* images in the semi-supervised learning setting: 63.5% with 1,464

strong annotations and 66.4% with 2,913 strong annotations. Remarkably, in this last *Semi (2,913)* experiment we exactly match the performance of the model trained with all 12,031 *trainval_aug* images strongly annotated.

We achieve our best result in the cross-dataset training scenario, using all available PASCAL and MS-COCO pixel-level annotations. This *Strong-Cross-Joint* result sets the new state-of-art on the official PASCAL VOC 2012 benchmark with 70.4% IOU, outperforming all previous publicly reported results by more than 3%.

4. Conclusions

The paper has explored the use of weak or partial annotation in training a state of art semantic image segmentation model. Extensive experiments on the challenging PASCAL VOC 2012 dataset have shown that: (1) Using weak annotation solely at the image-level seems insufficient to train a high-quality segmentation model. (2) Using weak bounding-box annotation in conjunction with careful segmentation inference for images in the training set suffices to train a competitive model. (3) Excellent performance is obtained when combining a small number of pixel-level annotated images with a large number of image-level annotated images in a semi-supervised setting, nearly matching the results achieved when all training images have pixel-level annotations. (4) Exploiting extra weak or strong annotations from other datasets can lead to large improvements.

Acknowledgments

We gratefully acknowledge the support of NVIDIA Corporation with the donation of GPUs used for this research.

References

- Chen, L.-C., Fidler, S., Yuille, A. L., and Urtasun, R. Beat the mturkers: Automatic image labeling from weak 3d supervision. In *CVPR*, 2014a.
- Chen, L.-C., Papandreou, G., Kokkinos, I., Murphy, K., and Yuille, A. L. Semantic image segmentation with deep convolutional nets and fully connected crfs. *arXiv:1412.7062*, 2014b.
- Cour, T., Sapp, B., and Taskar, B. Learning from partial labels. *JMLR*, 12:1501–1536, 2011.
- Dai, J., He, K., and Sun, J. Convolutional feature masking for joint object and stuff segmentation. *arXiv:1412.1283*, 2014.
- Deng, J., Dong, W., Socher, R., Li, L.-J., Li, K., and Fei-Fei, L. Imagenet: A large-scale hierarchical image database. In *CVPR*, 2009.
- Duygulu, P., Barnard, K., de Freitas, J. F., and Forsyth, D. A. Object recognition as machine translation: Learning a lexicon for a fixed image vocabulary. In *ECCV*, 2002.
- Eigen, D. and Fergus, R. Predicting depth, surface normals and semantic labels with a common multi-scale convolutional architecture. *arXiv:1411.4734*, 2014.
- Everingham, M., Eslami, S. M. A., Gool, L. V., Williams, C. K. I., Winn, J., and Zisserma, A. The pascal visual object classes challenge a retrospective. *IJCV*, 2014.
- Farabet, C., Couprie, C., Najman, L., and LeCun, Y. Learning hierarchical features for scene labeling. *PAMI*, 2013.
- Guillaumin, M., Küttel, D., and Ferrari, V. Imagenet auto-annotation with segmentation propagation. *IJCV*, 110(3):328–348, 2014.
- Hariharan, B., Arbeláez, P., Bourdev, L., Maji, S., and Malik, J. Semantic contours from inverse detectors. In *ICCV*, 2011.
- Hariharan, B., Arbeláez, P., Girshick, R., and Malik, J. Hypercolumns for object segmentation and fine-grained localization. *arXiv:1411.5752*, 2014.
- Hoffman, J., Guadarrama, S., Tzeng, E., Hu, R., Donahue, J., Girshick, R., Darrell, T., and Saenko, K. LSDA: Large scale detection through adaptation. In *NIPS*, 2014.
- Jia, Y., Shelhamer, E., Donahue, J., Karayev, S., Long, J., Girshick, R., Guadarrama, S., and Darrell, T. Caffe: Convolutional architecture for fast feature embedding. *arXiv:1408.5093*, 2014.
- Krähenbühl, P. and Koltun, V. Efficient inference in fully connected crfs with gaussian edge potentials. In *NIPS*, 2011.
- Kuck, H. and de Freitas, N. Learning about individuals from group statistics. In *UAI*, 2005.
- Lempitsky, V., Kohli, P., Rother, C., and Sharp, T. Image segmentation with a bounding box prior. In *ICCV*, 2009.
- Lin, T.-Y., Maire, M., Belongie, S., Hays, J., Perona, P., Ramanan, D., Dollár, P., and Zitnick, C. L. Microsoft coco: Common objects in context. In *ECCV*, 2014.
- Long, J., Shelhamer, E., and Darrell, T. Fully convolutional networks for semantic segmentation. *arXiv:1411.4038*, 2014.
- Lu, W.-L., Ting, J.-A., Little, J. J., and Murphy, K. P. Learning to track and identify players from broadcast sports videos. *PAMI*, 2013.
- Mostajabi, M., Yadollahpour, P., and Shakhnarovich, G. Feedforward semantic segmentation with zoom-out features. *arXiv:1412.0774*, 2014.
- Oquab, M., Bottou, L., Laptev, I., and Sivic, J. Weakly supervised object recognition with convolutional neural networks. In *NIPS*, 2014.
- Papandreou, G., Kokkinos, I., and Savalle, P.-A. Untangling local and global deformations in deep convolutional networks for image classification and sliding window detection. *arXiv:1412.0296*, 2014.
- Pathak, D., Shelhamer, E., Long, J., and Darrell, T. Fully convolutional multi-class multiple instance learning. *arXiv:1412.7144*, 2014.



Figure 7. Qualitative DeepLab-CRF segmentation results on the PASCAL VOC 2012 *val* set with the proposed training methods (see Sec. 3.7 for details). We show difficult examples in the last two rows.

- Pinheiro, P. and Collobert, R. Recurrent convolutional neural networks for scene labeling. In *ICML*, 2014a.
- Pinheiro, P. O. and Collobert, R. Weakly supervised semantic segmentation with convolutional networks. *arXiv:1411.6228*, 2014b.
- Rother, C., Kolmogorov, V., and Blake, A. Grabcut: Interactive foreground extraction using iterated graph cuts. In *SIGGRAPH*, 2004.
- Simonyan, K. and Zisserman, A. Very deep convolutional networks for large-scale image recognition. *arXiv:1409.1556*, 2014.
- Verbeek, J. and Triggs, B. Region classification with markov field aspect models. In *CVPR*, 2007.
- Vezhnevets, A. and Buhmann, J. M. Towards weakly supervised semantic segmentation by means of multiple instance and multitask learning. In *CVPR*, 2010.
- Vezhnevets, A., Ferrari, V., and Buhmann, J. M. Weakly supervised semantic segmentation with a multi-image model. In *ICCV*, 2011.
- Vezhnevets, A., Ferrari, V., and Buhmann, J. M. Weakly supervised structured output learning for semantic segmentation. In *CVPR*, 2012.
- Xia, W., Domokos, C., Dong, J., Cheong, L.-F., and Yan, S. Semantic segmentation without annotating segments. In *ICCV*, 2013.
- Xu, J., Schwing, A. G., and Urtasun, R. Tell me what you see and i will show you where it is. In *CVPR*, 2014.
- Zhu, J., Mao, J., and Yuille, A. L. Learning from weakly supervised data by the expectation loss svm (e-svm) algorithm. In *NIPS*, 2014.